IOSR Journal of Computer Engineering (IOSR-JCE)
e-ISSN: 2278-0661,p-ISSN: 2278-8727, Volume 23, Issue 6, Ser. III (Nov. –Dec. 2021), PP 10-25
www.iosrjournals.org

DSTATCOM Employing Gradient Descent Back Propagation with Momentum (GDBPM) Based $icos\phi$ Control Algorithm for Shunt Compensation

V RAMU
KUC,KOTTAGUDEM

P HARITHA
M.TECH,WITS COLLEGE

Abstract-*This paper focuses on model aspect and design of control algorithm for a three phase three wire (3P3W) distribution static compensator (DSTATCOM) employing GDBPM based* $icos\phi$ *algorithm. The proposed technique is implemented by mathematical analysis with suitable learning rate and momentum behaviour using MATLAB/Simulink.This algorithm follows the systematic procedure for the extraction of fundamental weighting values of both active and reactive power component of load currents which is needed for the generation of the reference currents smoothly.Harmonic mitigation,power factor correction,load balancing, voltage regulation and rating of Voltage Source Converter (VSC) are demonstrated under various loading conditions.The real time implementation of DSTATCOM is also carried out using Real time digital simulator (RTDS). Both MATLAB and RTDS comparative results demonstrate the effectiveness of theDSTATCOM with the proposed control algorithm to fulfil the requirementas followed by IEEE-519 and IEC-61000-3standard.*

Key words*—GDBPM control algorithm;* $os\phi$ *control algorithm; DSTATCOM; VSC.*

Abbreviations

v , v_{sb}, v_{sc} instantaneous voltage
u_{ap}, u , u_{cp}in-phase unit voltage template
u_{aq}, u_{bq}, u_{cq} quadrature unit voltage template
v_t PCC voltage or actual ac voltage
i , i_{lb} , i_{lc} load currents
Z_{ap}, Z_{bp}, Z_{cp} activation function of the active component
Z_{aq}, Z , Z_{cq}activation function of the reactive component
w_{ap}, w , w_{cp} updated weighted values of the active component
w_{aq}, w_{bq}, w_{cq} updated weighted values of the reactive component
w0 initial weightof the input layer
$w01$ initial weight of the hidden layer
μ rate of learning
α momentum constant
$w_p$weighted average of fundamental active component
$w_q$weighted average of fundamental reactive component
v_{de} dc voltage error
v_{dc} (ref)reference dc voltage
v_{dc} actual dc voltage
v_{te} ac voltage error
v_t (ref) reference ac voltage

$k_{pdp,dp}$ PI parameter in dc bus controller
$k_{pqq,qq}$ PI parameter in ac bus controller
k_1, k_2 scaling factor
i , i_{sb} , i_{sc} source current
i_{sap}, i_s , i_{scp} in-phase component of source current
i_s , i_{sbq} , i_{scq} quadrature component of source current
w_s , w_{sqt} total weighted value of active and reactive component
i^* , i^* , i^* reference source current

$sa\ sb\ sc$

I. Introduction

In present distribution system, the use of distributed flexible ac transmission system (DFACTS) controllers have overcome disadvantages of electromechanical based controllers such asless speed of operation, lower switching protection, VA burden, unidirectional feature, low efficiency due to high loss and unreliable etc. The DSTATCOM is one of shunt connected DFACTS devices which is used to absorbs or injects the reactive component of current through the interfacing inductors at the point of common coupling (PCC).Such controller is commonly referred to as ‘‘advanced static VAR Compensator’’ (ASVC) or static synchronous condenser (STATCON).This device is enough capable to provide suitable remedial measures and cost effective solution to the poor power quality faced by the distribution system[1]. In order to control the actual behaviour of DSTATCOM,various design and modelling of the controller techniques are such as power balance theory [2], instantaneous reactive power theory [3], synchronous reference frame (SRF) theory [4], synchronous detection (SD) theorem [5], $icos\phi$ control technique [6-7]are described in the cited literature.

Besides these, many neural network training based algorithm like neural network controller [8-15],neural network based signature recognition algorithm [11], intelligent neural network algorithm [12],Hopfield neural network [14], Generalized growing pruning-radial basis function(GGP-RBF) [15],Adaptive RBF [17-18],Back propagation algorithm [18-19] have been adopted.Among the many control algorithms, developed Neural Network techniques has some specific advantages like feedforward, supervised, reinforcement training and self- organisation principles etc. [12-24].This control algorithm is applied for several purposes such as the identification of image, mapping data, data analysis, industrial processes, seismic signal classification and correctionof power quality issues etc. So, neural network is also a feasible solution to analyse both the linear and nonlinear behaviour of the load in the distribution system. In view of the changing scenario under restructured power system, many researchers and scientistsare stepping forward to integrate soft computing techniques with conventional algorithmfor better performance as compared to simple conventional algorithm.

In this paper, a GDBPM based$icos\phi$ control algorithm is employed in a three phase two level DSTATCOM for the extraction of active component and reactive component weighted value of load current under both balanced and unbalanced nonlinear loads. Thisalgorithm comprises three stages of training weight such as input signals training, computation of error signals and correction of training weights bearing the various characteristics like Continuity, differentiability, structural flexibility, non-decreasing monotony and good representational capabilities are followed by this control technique. In actual practise, the concept of proposed control technique which is structured by mathematical analysisbased on the effect of GDBPM principle. In this application, source current harmonic reduction, Power factor improvement with dc voltage regulation of VSC, phase balancing and load compensation and rating of VSC are presented by using the proposed control technique under both balanced and unbalanced nonlinear loading conditions.

1. System Configuration Including Control Algorithm

The Fig.1 represents the schematic representation of power distribution system including proposed DSTATCOM.It consists three phase DSTATCOM, source and nonlinear load. The DSTATCOM is regarded as 3P3W two level VSC. Three interfacing impedances (a, Z_{cb}, Z_{cc}) are connected in series at the output of VSC to provide ripple free currents. The role of compensating currents (a, i_{cb}, i_{cc}) is to cancel the reactive power components and reduce the harmonics of source currents (i_{sa}, i_{sb}, i_{sc}) in the distribution system.

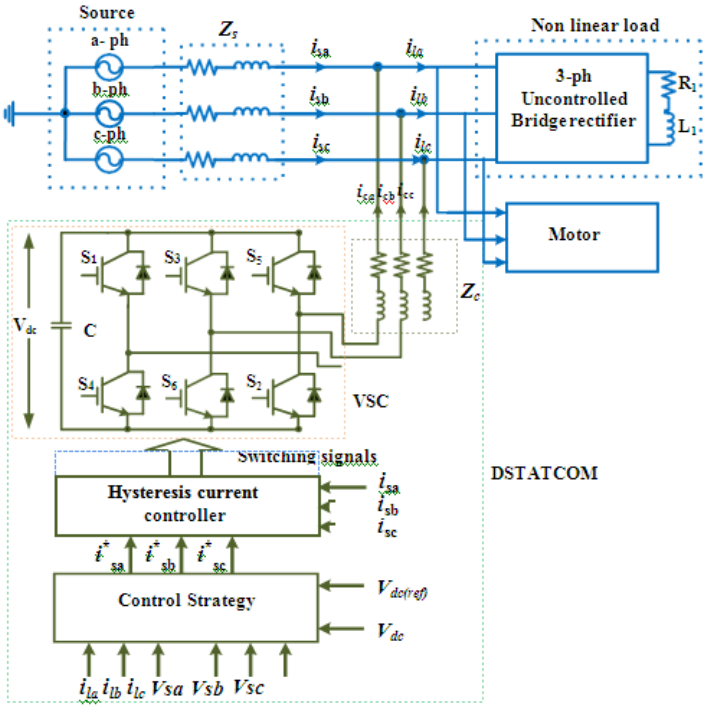

Fig.1 Schematic representation of the power distribution system including proposed DSTATCOM

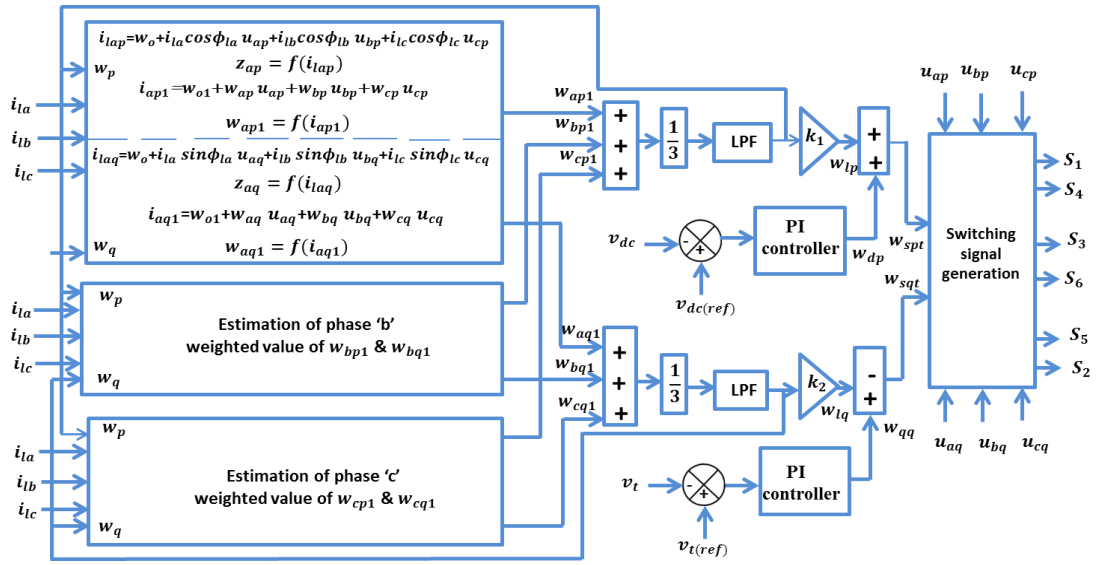

Fig.2 Block diagram for switching signals generation of VSC using GDBPM based$icos\phi$ control algorithm

The detail block diagram of GDBPM based $icos\phi$ control algorithm is shown in Fig.2. The proposed control technique is very robust by reducing the significant distortion of input quantity through its learning process. The complete algorithm involved in the estimation of switching signal generation is describedbelow.

A. Calculation of weighted value of fundamental active and reactive Components of load current

Both the updated weighted values of active and reactive power components are calculated using the GDBPMbased$icos\phi$control technique. This method is very efficient in updating the network weights and biases in the same direction of the performance function as shown in the Fig.3.

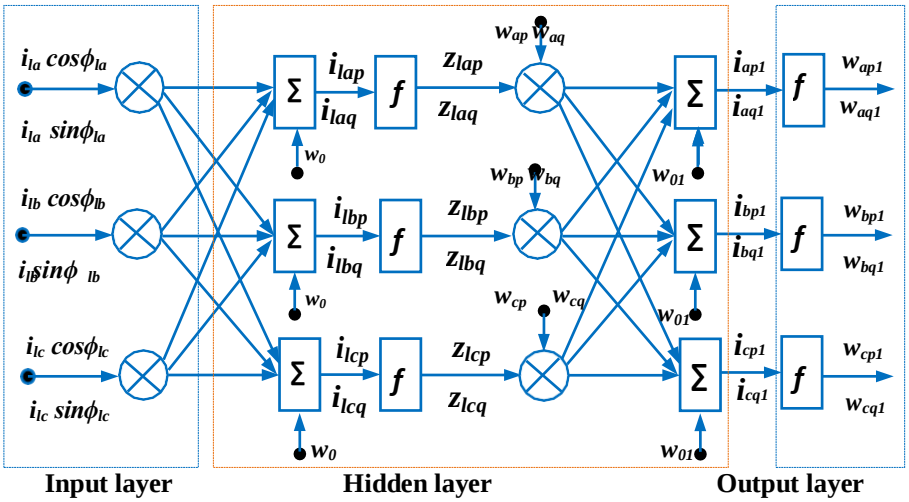

Fig.3 Estimation of weighted values using GDBPM based$icos\phi$control technique

Here, the weighted values of fundamental active components of the load currentsin input layer are given as

$il = w0 + ila\, cos\phi la\, uap + ilbcos\phi lbubp + ilc\, cos\phi lc\, ucp$ (1)

$il = w0 + ila\, cos\phi la\ uap + ilbcos\phi lbubp + ilc\, cos\phi lc\, ucp$ (2)

$il = w0 + ila\, cos\phi la\ uap + ilbcos\phi lb\, ubp + ilc\, cos\phi lc\, ucp$ (3)

In-phase unit templates are obtained from the following equations at the point of common coupling (PCC)

$$u_{ap} = \frac{v_{sa}}{v_t}$$
$$u_{bp} = \frac{v_{sb}}{v_t} \quad (4)$$
$$u_{cp} = \frac{v_{sc}}{v_t}\}$$

And the amplitude atthe PCC voltages is obtained as

$$v_t = \sqrt{\frac{2(v_{sa}^2 + v_{sb}^2 + v_{sc}^2)}{3}} \quad (5)$$

The above extracted three phase currents of (i_{lap}, i_{lbp} and i_{lcp}) are passed through the continuous sigmoid function. This function describesabouta mathematical representation having S-shape curve. If $i_{lap} \to +ve\ \infty$, $Z_{ap} = 1$and$i_{lap} \to -ve\ \infty$, $Z_{ap} = -1$so it can be regarded as activation function whose limit lies in between -1 to1.The output signals Z_{ap}, Z_{bp}andZ_{cp}act as input signal are processed through the hidden layer can be obtained by the following equations

$$Z_{ap} = (i_{lap}) = \frac{1}{1 + e^{-i_{lap}}}$$
$$Z_{bp} = (i_{lbp}) = \frac{1}{1 + e^{-i_{lbp}}} \quad (6)$$
$$Z_{cp} = f(i_{lcp}) = \frac{1}{1 + e^{-i_{l}}}\}$$

The three phase fundamental component outputs of this layer (i_{ap1}, i_{bp1} andi_{cp1}) are expressed as

$$i_{ap1} = w_{01} + w_{ap}Z_{ap} + w_{bp}Z_{bp} + w_{cp}Z_{cp} \quad (7)$$
$$i_{bp1} = w_{01} + w_{ap}Z_{ap} + w_{bp}Z_{bp} + w_{cp}Z_{cp} \quad (8)$$
$$i_{cp1} = w_{01} + w_{ap}Z_{ap} + w_{bp}Z_{bp} + w_{cp}Z_{cp} \quad (9)$$

The drawbacks of GDBP are overcome by GDBPM algorithm. In this proposed algorithm, the concept of momentum is included. The momentumallows not only to the gradient but also weight changes.So that weight updation will not be stuck in local minimum. It allows weight update which ismediated by a momentum constant'α'. The updated weight$w_{ap}$of active component for phase-a can be expressed as

$$w_{ap} = + \mu\{w_p - w_{ap1}\}f'(i_{ap1}) + \alpha\, w_{p-1} \quad (10)$$

Where w_{ap1} is the a-phase fundamental weighted value of the active component, $f'(i_{ap1})$ is the first derivative of i_{ap1}component,and w_{p-1} is the previous value average weighted value of the active component etc.

Similarly, the updated weight for b-phase and c-phase can be expressed as

$$w = w_p + \mu\{w_p - w_{bp1}\}f'(i_{bp1}) + \alpha\, w_{p-1} \quad (11)$$
$$w = w_p + \mu\{w_p - w_{cp1}\}f'(i_{cp1}) + \alpha\, w_{p-1} \quad (12)$$

The fundamental values i_{ap1}, i_{bp1} andi_{cp1} are processed through the sigmoid function act as an activation function can be expressed in terms of w_{ap1}, w_{bp1}&w_{cp1} as

$$w_{ap1} = (i_{ap1}) = \frac{1}{1 + e^{-i_{ap1}}}$$
$$w_{bp1} = (i_{bp1}) = \frac{1}{1 + e^{-i_{bp1}}} \quad (13)$$
$$w_{cp1} = f(i_{cp1}) = \frac{1}{1 + e^{-i_{cp1}}}\}$$

The weighted average of fundamental active component can be calculated as

$$w_p = \frac{w_{ap1} + w_{bp1} + w_{cp1}}{3} \tag{14}$$

The low frequency components are separated by using 1st order low-pass filters (LPF).This extracted active power components is reduced by a linearized scaled factor "k_1" to get the actual value (w_{lp})which is shown in Fig. 2. Similarly, the weighted values of thereactive components of the load currentin the input layer are given as

$$i_l = w_0 + i_{la} sin\phi_{la}\, u_{aq} + i_{lb} sin\phi_{lb}\, u_{bq} + i_{lc} sin\phi_{lc}\, u_{cq} \tag{15}$$

$$i_l = w_0 + i_{la}\, sin\phi_{la}\, u_{aq} + i_{lb} sin\phi_{lb}\, u_{bq} + i_{lc}\, sin\phi_{lc}\, u_{cq} \tag{16}$$

$$i_{lcq} = w_0 + i_{la}\, sin\phi_{la}\, u_{aq} + i_{lb} sin\phi_{lb}\, u_{bq} + i_{lc}\, sin\phi_{lc}\, u_{cq} \tag{17}$$

The quadrature unit voltage template of a, b & c-phaseare expressed as

$$\left.\begin{aligned} u_{aq} &= \frac{u_{bp} + u_{cp}}{\sqrt{3}} \\ u_{ba} &= \frac{3u_{ap} + u_{bp} - u_{cp}}{2\sqrt{3}} \\ u_{cq} &= \frac{-3u_{ap} + u_{bp} - u_{cp}}{2\sqrt{3}} \end{aligned}\right\} \tag{18}$$

The above weighted values of i_l, i_{lba} &i_{lca} are passed through the sigmoid function for the estimation of three weighted values of reactive component of load currents Z_{aq}, Z_{bq}&Z_{cq} which can be expressed by the following equations

The above weighted values of i_l, i_{lba} &i_{lca} are passed through the sigmoid function for the estimation of three weighted values of reactive component of load currents Z_{aq}, Z_{bq}&Z_{cq} which can be expressed by the following equations

$$\left.\begin{aligned} Z_{aq} = (i_{laq}) &= \frac{1}{1 + e^{-i_{laq}}} \\ Z_{bq} = (i_{lb}) &= \frac{1}{1 + e^{-i_{lbq}}} \\ Z_{cq} = (i_{lcq}) &= \frac{1}{1 + e^{-i_l}} \end{aligned}\right\} \tag{19}$$

The Z_{aq}, Z_{bq}&Z_{cq}acts as input signals are processed through the hidden layer. The three phase fundamental output components of this layer i_{aq1}, i_{bq1}&i_{cq1} are expressed as

$$i_{aq1} = w_{01} + w_{aq}Z_{aq} + w_{bq}Z_{bq} + w_{cq}Z_{cq} \tag{20}$$

$$i_{bq1} = w_{01} + w_{aq}Z_{aq} + w_{bq}Z_{bq} + w_{cq}Z_{cq} \tag{21}$$

$$i_{cq1} = w_{01} + w_{aq}Z_{aq} + w_{bq}Z_{bq} + w_{cq}Z_{cq} \tag{22}$$

Here w, w_{bq} and$w_{cq}$are updated weighting values of reactive component of the load current in a, b and c-phase used as feedback signal respectively.

The updated weight "w_{aq}"of reactive component of a-phase can be expressed as

$$w = w_q + \mu\{w_q - w_{aq1}\}f'(i_{aq1}) + \alpha\, w_{q-1} \tag{23}$$

Where$w_{aq1}$is the a-phase fundamental weighted amplitude of the reactive component, $f'(i_{aq1})$ is the first derivative of i_{aq1}component and w_{q-1} is the previous value average weighted value of the reactive component etc.

Similarly the two equations for b and c-phase can be expressed as

$$w = w_q + \mu\{w_q - w_{bq1}\}f'(i_{bq1}) + \alpha\, w_{q-1} \tag{24}$$

$$w_{cq} = + \mu\{w_q - w_{cq1}\}f'(i_{cq1}) + \alpha\, w_{q-1} \tag{25}$$

The fundamental values i_{aq1}, i_{bq1}&i_{cq1} are processed through the sigmoid function act as an activation function can be expressed in terms of w_{aq1}, w_{bq1}andw_{cq1} as

$$w_{aq1} = (i_{aq1}) = \frac{1}{1 + e^{-i_{aq1}}}$$
$$w_{bq1} = (i_{bq1}) = \frac{1}{1 + e^{-i_{bq1}}} \quad (26)$$
$$w_{cq1} = (i_{cq1}) = \frac{1}{1 + e^{-i_{cq1}}} \}$$

The weighted average of fundamental reactive component can be calculated as

$$w_q = \frac{w_{aq1} + w_{bq1} + w_{cq1}}{3} \quad (27)$$

The low frequency components are separated by using 1st-order low-pass filters (LPF).This extracted reactive power components of current is reduced by a linearized scaled factor "k_2" the actual value (w_{lq})which is shown in Fig. 2. To ensure the stability margin of the closed-loop control systems, two linearizing factors k_1 and k_2 are used while extracting both direct and quadrature axis weighted values, which are followed by low pass filter. This filter allows preserving the system dynamics at low frequency and rejects the noise. By maintaining so, the corresponding apparel advantages are obtained; generation of reference signal are sensed with higher accuracy and one cycle control in updating the weighted values closer to target value at a faster rate.

B. Estimation of the active component of reference source currents

The difference between reference dc voltage and actual dc voltage is the error in dc voltage (v_{de}) can be expressed as

$$v = v_{dc\,(ref)} - v_{dc} \quad (28)$$

This difference is processed through the Proportional-Integral (PI) controller to regulate the constant dc bus voltage. The output of PI controller can be expressed as

$$w = k_{pdp} v_{de} + k_{idp} \int v_{de} dt \quad (29)$$

The sum of output of PI controller and the average magnitude of active component is the total active components of the reference source current can be expressed as

$$w_s = w_{dp} + w_{lp} \quad (30)$$

C. Estimation of the reactive component of reference source currents

The difference in between reference ac bus voltage and actual ac bus voltage is the error in ac voltage (v_{te}) can be expressed as

$$v = v_{t\,(ref)} - v_{ta} \quad (31)$$

This difference is processed through the PI controller to regulate the constant ac bus voltage. The output of PI controller can be expressed as

$$w_{qq} = {}_{qq} v_{te} + k_{iqq} \int v_{te} dt \quad (33)$$

D. Estimation of switching signal generation

Three phase instantaneous reference source active component are estimated by multiplying in phase unit voltage template and active power current component and these are obtained as

$$i_{sap} = w_{spt} u_{ap}$$
$$i_s = w_{spt} u_{bp} \} \quad (34)$$
$$i_{scp} = w_{spt} u_{cp}$$

Similarly, three phase instantaneous reference source reactive component are estimated by multiplying quadrature unit voltage template and reactive current component and these are obtained as

$$i_{saq} = w_{sqt} u_{aq}$$
$$i_s = w_{sqt} u_{bq} \} \quad (35)$$
$$i_{scq} = w_{sqt} u_{cq}$$

The summation of active and reactive components of respective phase is called as reference source currents and are obtained as

$$i^*_{sa} = i_{sap} + i_{saq}$$
$$i^*_{sb} = i_{sbp} + i_s \} \quad (36)$$
$$i^*_{sc} = i_{scp} + i_{scq}$$

The both actual source currents ($i_{sa,b}, i_{sc}$) and the reference source currents ($i^*_{sa}, i^*_{sb}, i^*_{sc}$) of the respective phases are compared then current error signals are fed to a Hysteresis current controllers (HCC). Their outputs are used to feed the insulated-gate bipolar transistors (IGBTs) s_1 to $s_6$of the VSC served as a DSTATCOM.

II. Results And Discussion

GDBPM based $icos\phi$ control technique is employed in the DSTATCOM and the comparative performance are demonstrated under balanced and unbalanced loading conditions using MATLAB/SIMULINK.

i. System performance including DSTATCOM controlled by GDBP based$icos\phi$ algorithm under balanced condition of rectifier loading

The distribution system performance including DSTATCOMcontrolled by GDBPM based $icos\phi$ algorithm under the balanced loading is performed. The corresponding simulation waveforms of capacitor voltage (v_{dc}),compensating current (i_{ca}, i_{cb}, i_{cc}), load current (i_{la} , i_{lb}, i_{lc}), source current (i_S)and source voltage (v_S)are shown in fig.4(a).The harmonic spectrum of source current of all phases are shown in fig. 4(b), 4(c) and 4(d) respectively indicates the harmonics reduction. Similarly, the harmonic spectrum of load current of all phases are shown in fig. 4(e), 4(f) and 4(g) respectively. which indicates no control over load current harmonics reduction followed by this algorithm, are summarized in table:1. As depicted in Fig. 4(h), supply voltage and source current are balanced and sinusoidal, shows power factor correction. The obtained voltage across the self-supported capacitor is 577V, achieve the load compensation. Rating of VSC is 7.006 kVAR which is evaluated by considering dc link capacitor and compensator current.

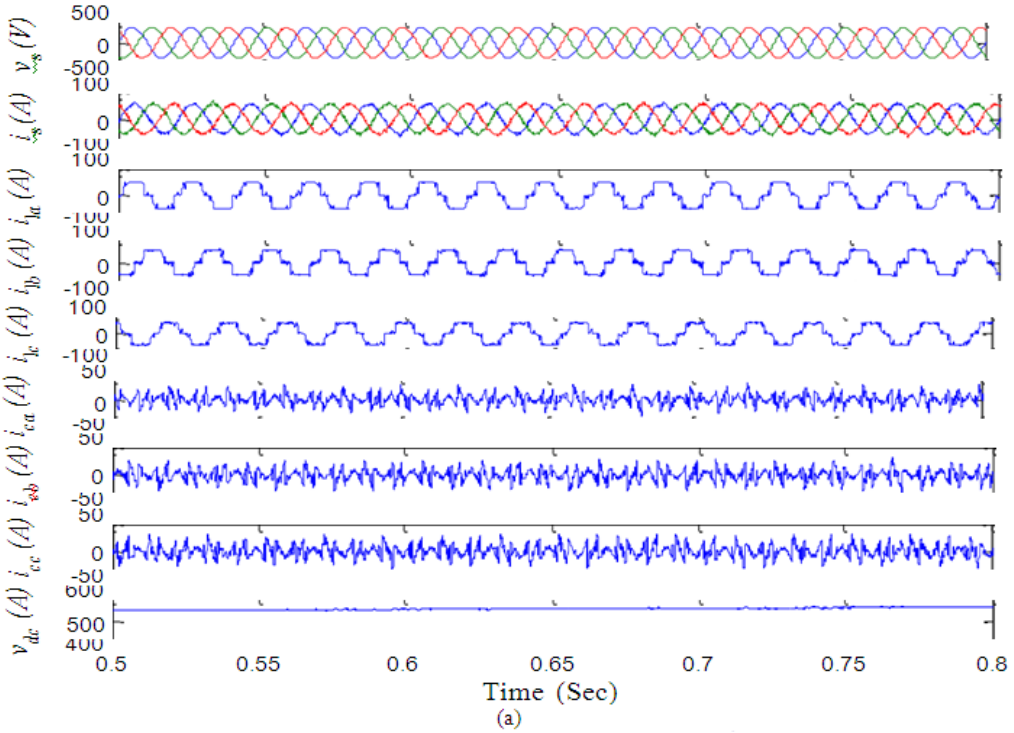

(a)

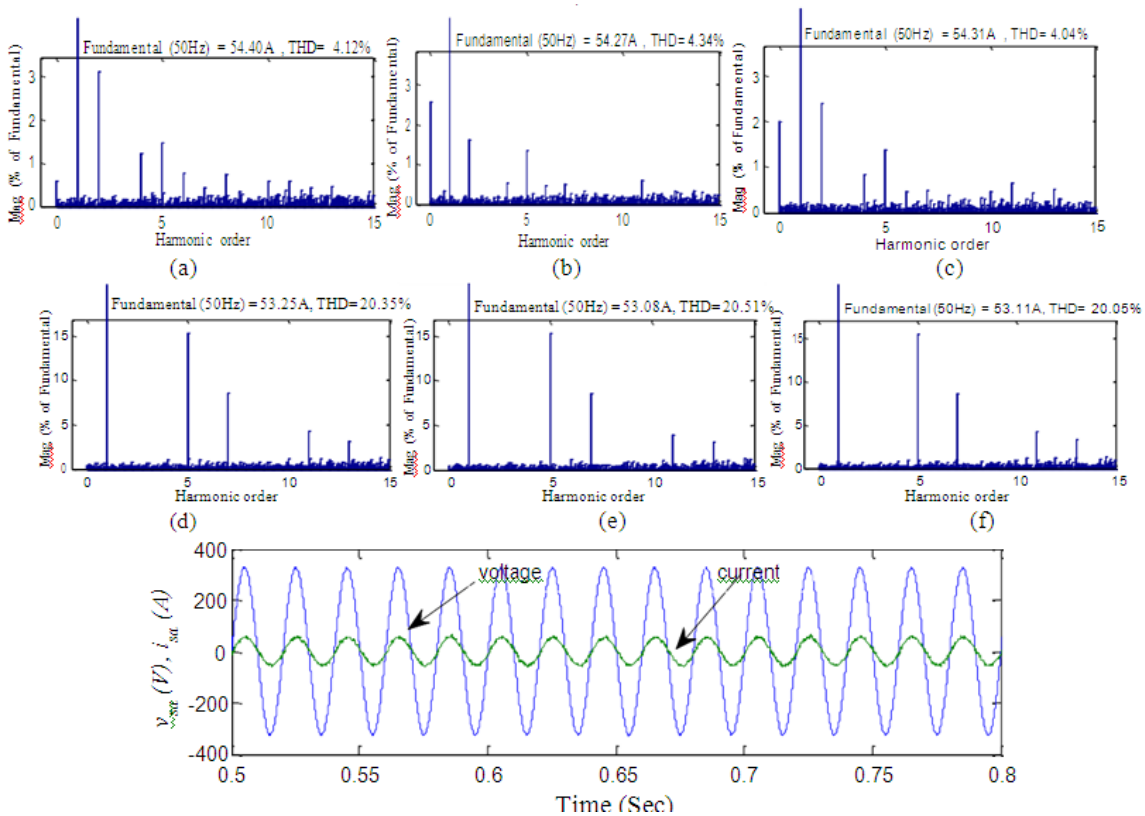

Fig. 4 (a) System performance including DSTATCOM using GDBPM based$icos\phi$ control algorithm under balanced loading (b) Harmonic spectra of source current of phase-a (c) Harmonic spectra of source current of phase-b (d) Harmonic spectra of source current of phase-c (e) Harmonic spectra of load current of phase-a (f) Harmonic spectra of load current of phase-b (g) Harmonic spectra of load current of phase-c and (h) source voltage and source current of phase-a.

i. System performance including DSTATCOM controlled by GDBPM based $icos\phi$ algorithm under unbalanced condition of rectifier loading

The distribution system performance including DSTATCOM controlled by GDBPM based $icos\phi$ algorithm under the unbalanced loading is performed. Such situation is created by removing a-phase load between 0.6 to 0.7 sec. The

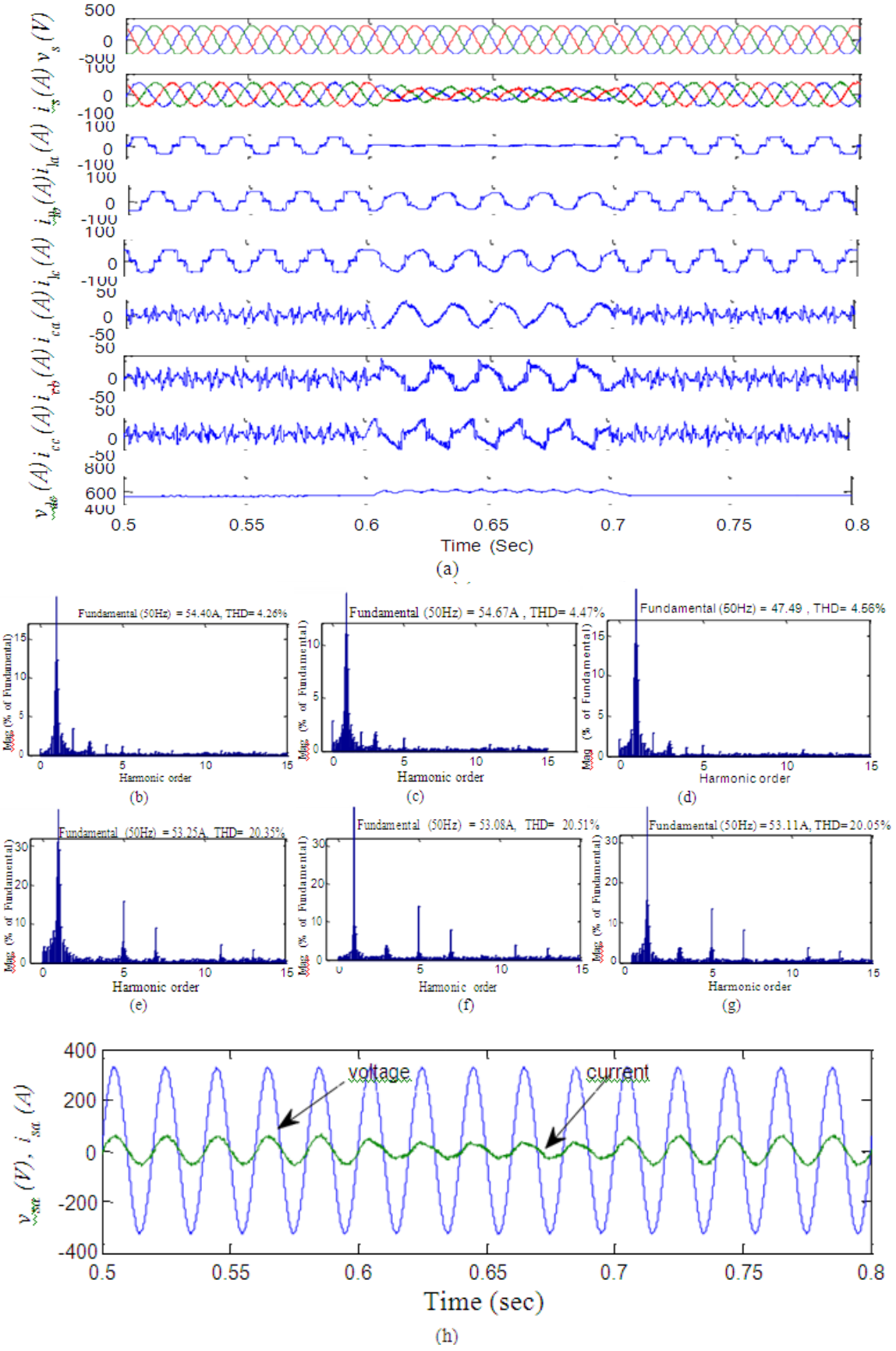

Fig. 5 (a)System performance including DSTATCOM using GDBPM based *icosϕ* control algorithm under un-balanced loading,(b) Harmonic spectra of source current of phase-a (c) Harmonic spectra of source current of

phase-b (d) Harmonic spectra of source current of phase-c (e) Harmonic spectra of load current of phase-a (f) Harmonic spectra of load current of phase-b (g) Harmonic spectra of load current of phase-c and (h) source voltage and source current of phase-a.

corresponding simulation waveforms of capacitor voltage (v_{dc}), compensating current (i_{ca}, i_{cb}, i_{cc}), load current (i_{la} , i_{lb}, i_{lc}), source current (i_s) and source voltage (v_s)are shown in fig.5(a).The harmonic spectrum of source current of all phases are shown in fig. 5(b), 5(c) and 5(d) respectively indicates the harmonics reduction. Similarly, the harmonic spectrum of load current of all phases are shown in fig. 5(e), 5(f) and 5(g) respectively. which indicates no control over load current harmonics reduction followed by this algorithm, are summarized in table:1. As depicted in Fig. 5(h), supply voltage and source current are balanced and sinusoidal, shows power factor correction.The obtained voltage across the self-supported capacitor varies from 600-629V instead of maintaining is 577V during this condition to achieve the load compensation.

iii. System performance including DSTATCOM controlled by GDBP based icosϕ algorithm under balanced condition of both rectifier and motor loading

The distribution system performance including DSTATCOM controlled by GDBP based $icos\phi$ algorithm under the balanced loading is performed. Here, one is uncontrolled rectifier feeding to R-L load and other one is motor load. Both these load under throughtout time of an interest remain constant. The corresponding simulation waveforms of capacitor voltage (v_{dc}), compensating current (i_{ca}, i_{cb}, i_{cc}), load current (i , i_{lb}, i_{lc}), source current (i_s) and source voltage (v_s)are shown in fig.6(a). The harmonic spectrum of source current of all phases are shown in fig. 6(b), 6(c) and 6(d) respectively indicates the harmonics reduction. Similarly, the harmonic spectrum of load current of all phases are shown in fig. 6(e), 6(f) and 6(g) respectively. which indicates no control over load current harmonics reduction followed by this algorithm, are summarized in table:1. As depicted in Fig. 6(h), supply voltage and source current are balanced and sinusoidal, shows power factor correction. The fast acting response of DSTATCOM are resulted by the compensator current of all phases. The obtained voltage across the self-supported capacitor is 577V, achieve the load compensation. Rating of VSC is 7.006 kVAR which is evaluated by considering dc link capacitor and compensator current.

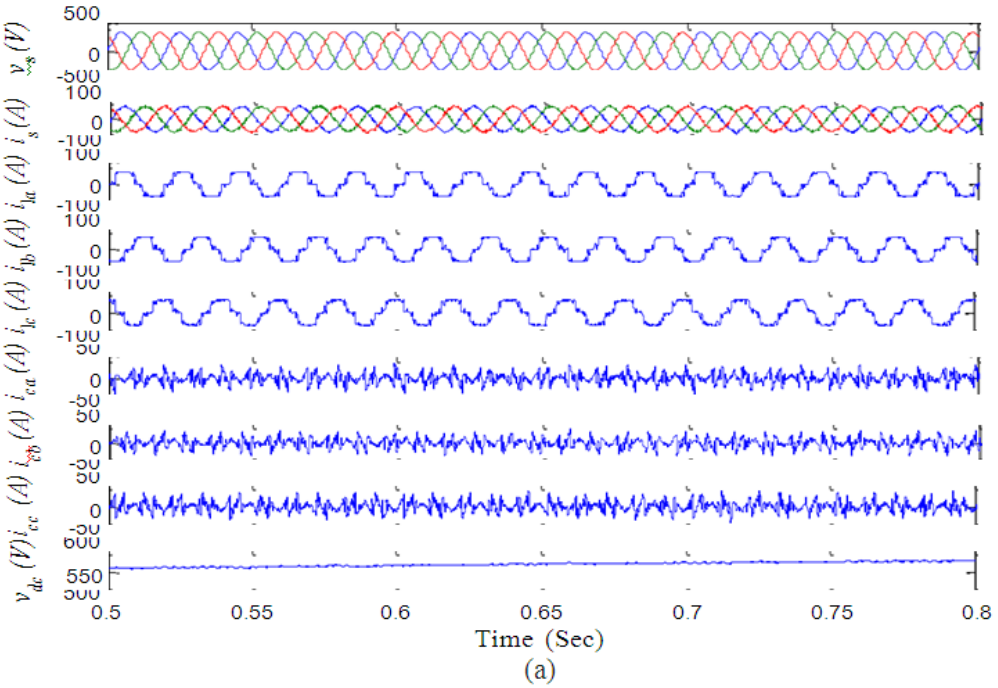

(a)

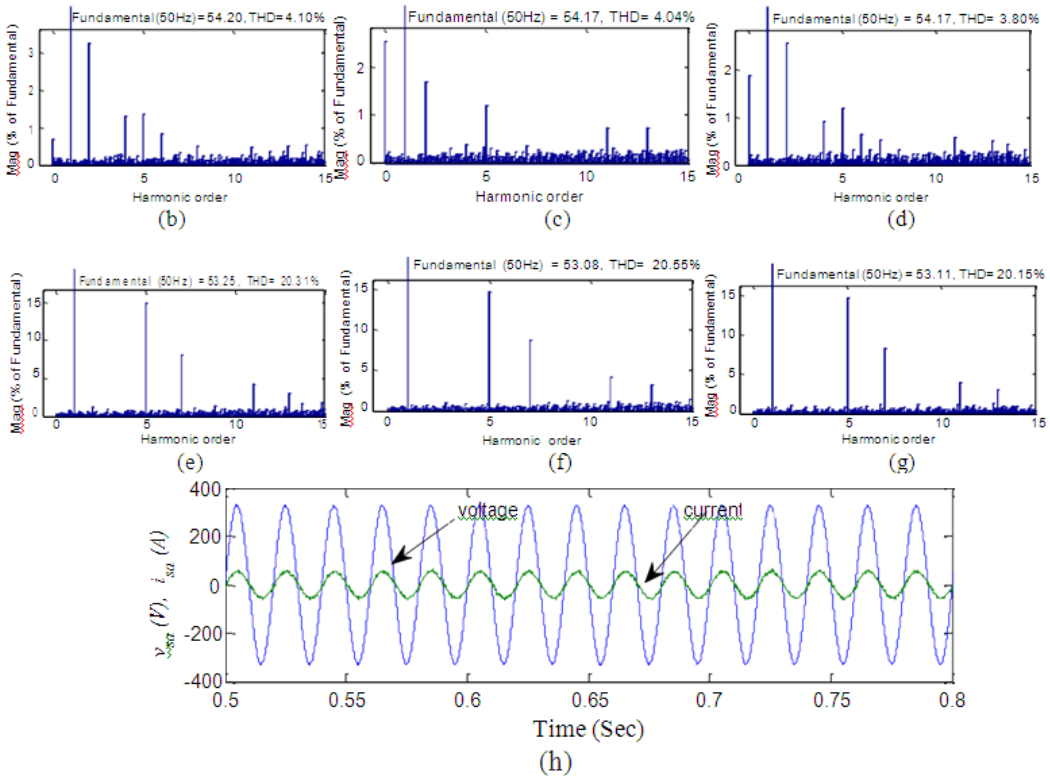

Fig. 6(a) System performance including DSTATCOM using GDBPM based $icos\phi$ control algorithm under balanced loading, (b) Harmonic spectra of source current of phase-a, (c) Harmonic spectra of source current of phase-b, (d) Harmonic spectra of source current of phase-c, (e)

Harmonic spectra of load current of phase-a, f. Harmonic spectra of load current of phase-b, (g) Harmonic spectra of load current of phase-c and (h). source voltage and source current of phase-a.

iii. System performance including DSTATCOM controlled by GDBPM based $icos\phi$ algorithm under unbalanced condition of rectifier and balanced motor loading

The distribution system performance including DSTATCOM controlled by GDBPM based $icos\phi$ algorithm under the unbalanced loading is performed. Here, one is uncontrolled rectifier feeding to R-L load and other one is motor load. Such situation is created by removing a-phase load of uncontrolled rectifier feeding to the R-L load between
0.6 to 0.7 sec. The other motor load under throughtout time of an interest remain constant. The corresponding simulation waveforms of capacitor voltage (v_{dc}), compensating current (i_{ca}, i_{cb}, i_{cc}), load current (i , i_{lb}, i_{lc}), source current (i_s) and source voltage (v_s) are shown in fig.7(a). The harmonic spectrum of source current of all phases are shown in fig. 7(b), 7(c) and 7(d) respectively indicates the harmonics reduction. Similarly, the harmonic spectrum of load current of all phases are shown in fig. 7(e), 7(f) and 7(g) respectively. which indicates no control over load current harmonics reduction followed by this algorithm. As depicted in Fig. 7(h), supply voltage and source current are balanced and sinusoidal, shows power factor correction. The fast acting response of DSTATCOM is resulted by the compensator current of all phases. The obtained voltage across the self-supported capacitor varies from 600- 629V instead of maintaining is 577V during this condition to achieve the load compensation.

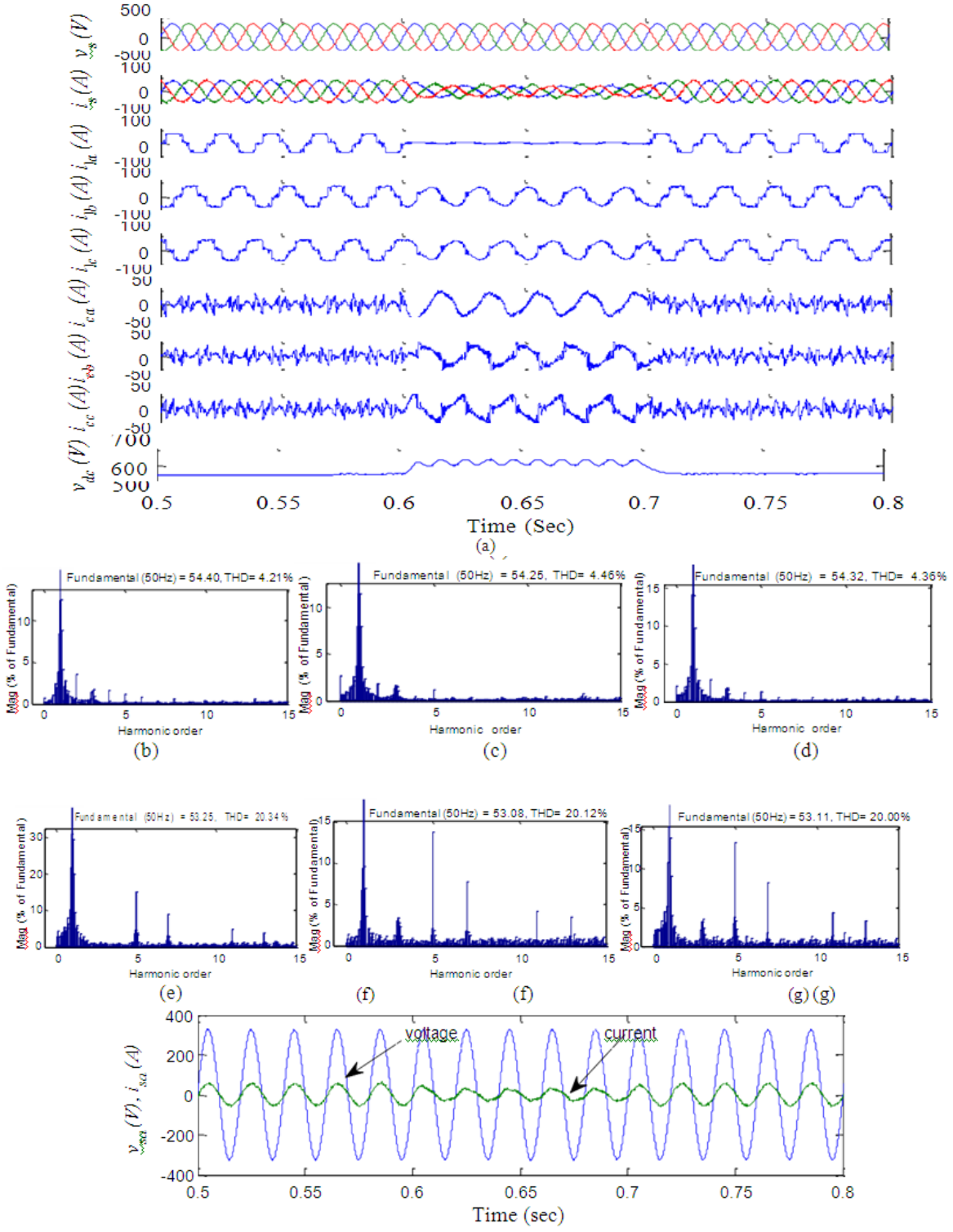

Fig.7 a.System performance including DSTATCOM using GDBPM based $icos\phi$ control algorithm under un balanced loading, b.Harmonic spectra of source current of phase-a, c. Harmonic spectra of source current of phase-b, d. Harmonic spectra of source current of phase-c, e. Harmonic spectra of load current of phase-a, f. Harmonic spectra of load current of phase-b, g. Harmonic spectra of load current of phase-c and h. source voltage and source current of phase-a.

Table:1 THD% of supply current, PCC voltage and load current

System configuration	i_{sa}	i_{sb}	i_{sc}	v_{la}	v_{lb}	v_{lc}	i_{la}	i_{lb}	i_{lc}
	Amp, % THD			Volt, % THD			Amp, % THD		
Case:i	54.40, 4.12	54.27, 4.34	54.31, 4.04	294.40, 12.85	294.4, 12.67	294.6, 12.51	53.25, 20.35	53.08, 20.51	53.11, 20.05
Case:ii	54.40, 4.26	54.67, 4.47	54.35, 4.56	294.38, 12.87	294.2, 12.72	294.5, 12.47	53.25, 20.35	53.08, 20.51	53.11, 20.05
Case:iii	54.20, 4.10	54.17, 4.04	54.17, 3.80	294.40, 12.85	294.4, 12.67	294.6, 12.51	53.25, 20.31	53.08, 20.55	53.11, 20.15
Case:iv	54.40, 4.21	54.25, 4.46	54.32, 4.36	294.38, 12.87	294.2, 12.72	294.5, 12.47	53.25, 20.34	53.08, 20.12	53.11, 20.00

With these discussions made above, another prime concern in deciding rating of DSTATCOM has to be considered. Reduced rating of DSTATCOM means reduced rating of VSC. Though the rating of VSC is directly proportional to the v_{dc}. So that less amount of v_{dc}can be preferable for selection of reduced rating of DSTATCOM. It confirms the suggested algorithm is more prominent than other for the better performance of DSTATCOM in the distribution system, followed by IEEE grid codes for power quality issues.

To access the performance, the controller having the simulation time is set at 1Sec. But, convergence characteristics are observed by GDBPM based icosϕ at 0.05Sec. From this one can be chosen, the proposed approach is having quick convergence and less computational complexity compared to the icosϕ technique.

The objective of new controller design is to generate the accurate and precise reference source current for DSTATCOM. Furthermore, reference source current is dependent on the fundamental active and reactive component of the load current. In order to have the extract filtered and tuned weight, GDBPM based icosϕ is employed and formulated by mathematical analysis. Then the current errors (i.e. the difference between reference source current and actual source current) is governed by hysteresis current controller (HCC). Hence switching pulses are generated and help to inject the appropriate compensator current at the PCC. The observation is made from both the simulation study, the weight obtained from the GDBPM based icosϕ technique has less static error, faster convergence and less affected by noise. Hence, better source current harmonic reduction, power factor improvement, voltage regulation and load balancing are achieved than other one.

III. Experimental Results

RT-LAB allows the user to readily convert Simulink models, via Real-time workshop (RTW), and then to conduct Real-time simulation of those models executed on multiple target computers equipped with multi-core PC processors. This is used particularly for hardware in the loop and rapid control prototyping applications. RT-LAB transparently handles synchronization, user interaction, real world interfacing using I/O boards and data exchanges for seamless distributed execution. The OP5142 is one of the key building blocks in the modular OP5000 I/O system from Opal- RT Technologies. It allows the incorporation of FPGA technologies in RT-LAB simulation clusters for distributed execution of HDL (Hardware description language) functions and high-speed, high-density digital I/O in real-time models. Based on the highest density Xilinx Spartan-3 FPGAs, the OP5142 can be attached to the backplane of an I/O module of either a Wanda 3U- or Wanda 4U-based Opal-RT simulation system. It communicates with the target PC via a PCI-Express (Peripheral Component Interconnect - Express) ultra-low- latency real-time bus interface .

Simulations are carried out to show the system performances including DSTATCOMcontrolled by using GDBPM based $icos\phi$ algorithm under different loading conditions. The following analysis are obtained in a PCinstalled with Opal RT-Lab software in real time [21-25]. The Opal RT-Lab simulation waveforms are obtained using digital storage oscilloscope (DSO) and these are presented in figs.8 to 11.

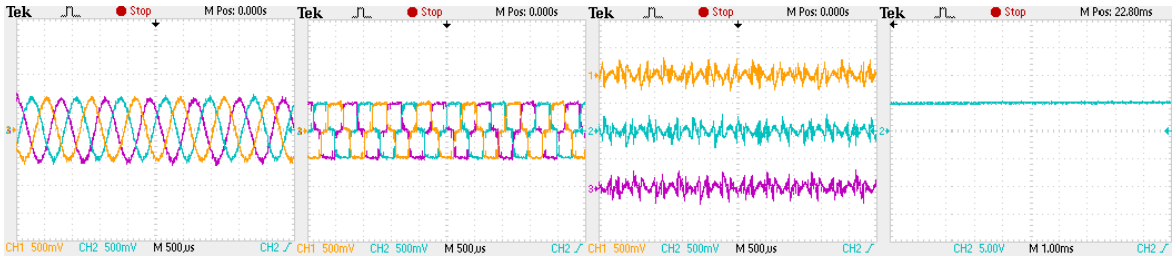

(a) (b) (c) (d)

Fig.8 RT-Lab simulation waveform for DSTATCOM using GDBPM based $icos\phi$ technique under balancedcondition of rectifier loading (a) source current, (b) load current, (c) compensated current and (d) dc link voltage.

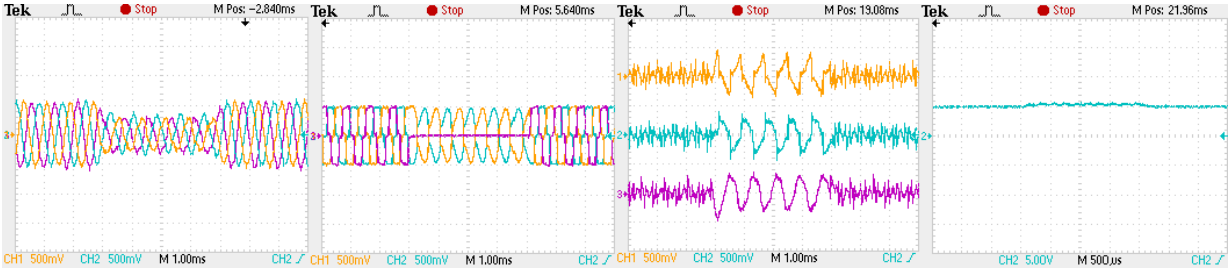

(a) (b) (c) (d)

Fig.9 RT-Lab simulation waveform for DSTATCOM using GDBPM based *icosϕ* technique under under unbalanced condition of rectifier loading (a) source current, (b) load current, (c) compensated current and (d) dc link voltage.

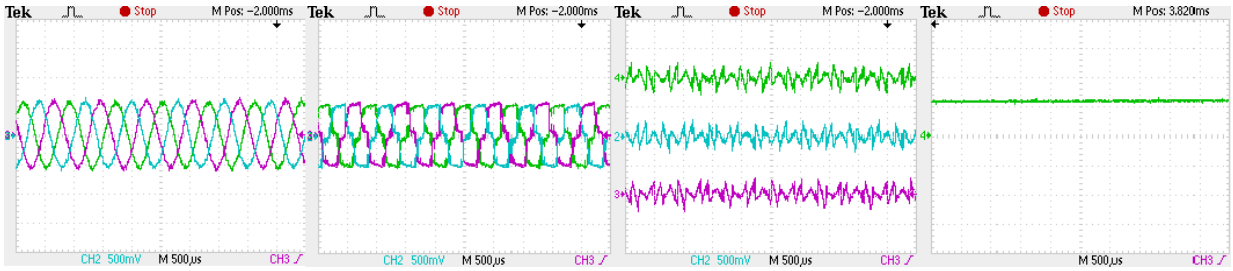

(a) (b) (c) (d)

Fig.10 RT-Lab simulation waveform for DSTATCOM using GDBP based *icosϕ* technique under both balanced condition of rectifier and motor loading (a) source current (50A/div), (b) load current (50 A/div), (c) compensated current (50 A/div) and (d) dc link voltage (500V/div).

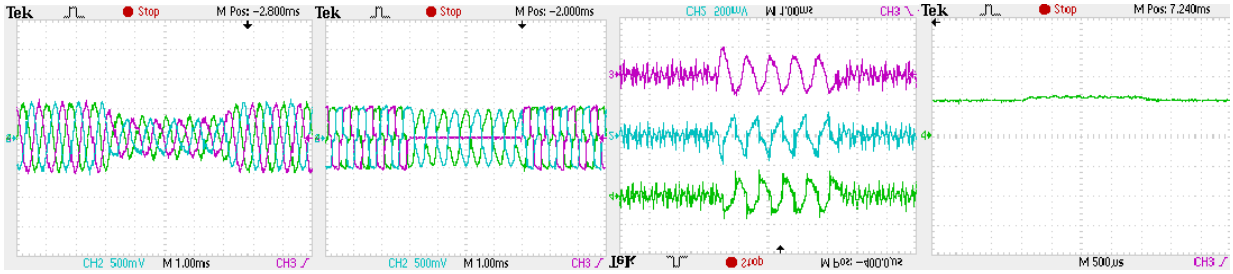

(a) (b) (c) (d)

Fig.11 RT-Lab simulation waveform for DSTATCOM using GDBP based *icosϕ* technique under unbalanced rectifier loading and balanced motor loading (a) source current (50A/div), (b) load current (50 A/div), (c) compensated current (50 A/div) and (d) dc link voltage (500V/div).

The scale is used for (i) source current (50A/div), (ii) load current (50A/div), (iii) compensated current (50A/div) and (iv) dc link voltage (500V/div).
The real time digital simulation results are in line with the simulation results and so confirm the superior performance of the GDBPM controlled *icosϕ* technique based DSTATCOM.
The various block parameters utilized for the purpose of simulation studies are shown illustrated in the Appendix.

IV. Conclusion

This paper has introduced and discussed on systematic design and operation of DSTATCOM using GDBPM based *icosϕ* control algorithm under both balanced and unbalanced loading condition.In this control technique, the previous weight is allowed to have new weight mediated by momentum constant successfully. It is concluded from the simulation studies that the % THD of source currents are 4.12, 4.34, 4.04 and 4.26, 4.47, 4.54 of phase a,phase b, phase c using proposed control technique under case iii and case iv respectively, whereas as that the % THD of source currents are 4.10, 4.44, 3.80 and 4.21, 4.46, 4.36 of phase a, phase b, phase c using proposed control technique under case vii and case viii respectively shown in table:1. This topology is capable of better shunt compensation including harmonic mitigation, power factor correction, load balancing and voltage regulation as recommendations governed by IEEE 519-1992 standard than the other

conventional method. Effectiveness of the MATLABsimulation results has been validated through Real-time lab simulation results.

Appendix:

Ac supply source: three phase 230 V (Line-Line), 50 Hz, Source resistor: $= 0.04\ \Omega$ and Source inductor: $L_S =$ 0.04 mH,Nonlinear load: three phase full bridge uncontrolled rectifier with R=13Ω and L= 200mH, Dynamic moto load 325V (L-L), 0.75kW and 0.75kVAR, Reference DC voltage $v_{dc}\,(ref)$ =700V, Reference AC voltage $v_t\ (ref)$=325V, Interfacing inductor L_f=1.5mH, Interfacing resistor$R_S = 0.04\ \Omega$, initial weight $w0 = 0.4$ and $w01 = 0.2$, Learning rate μ=0.6,$k1 = 0.4$,$k2 = 0.1$, α is the momentum constant,Cut of frequency of LPF in the DC bus controller=10 Hz, Cut of frequency of LPF in the AC bus controller=10 Hz, PI controller gain in the DC side $k_{pdp} = 2$, $k_{idp} = 3.5$, self-supported Capacitor=2000μF.

References

[1]. A Ghosh and GLedwich. Power quality enhancement using custom power devices. Norwell: Kluwer; 2002.

[2]. B.N. Singh, "Design and digital implementation of active filter with power balance theory,"*IEEE Proceedingon Electrical Power Application*,vol. 152, no. 5, pp. 1149–1160,2005.

[3]. MIM Montero, ERCadaval and FB Gonzalez,"Comparison of control strategies for shunt active power filters in three-phase four-wire systems,"*IEEE Transaction on Power Electronics*, vol. 22, no. 1, pp. 229–236,2007.

[4]. MAredes, HAkagi, EHWatanabe, EVSalgado and LFEncarnacao, "Comparisons between the p-q and p-q-r theories in three-phase four- wire systems,"*IEEE Transaction on Power Electronics*, vol. 24, no. 4, pp. 924–933,2009.

[5]. B Singh, P Jayaprakash, DPKothari, "New control approach for capacitor supported DSTATCOM in three-phase four wire distribution system under non-ideal supply voltage conditions based on synchronous reference frame theory,"*International Journal of Electrical Power & Energy Systems*, vol. 35, no. 5, pp. 1109–1117,2011.

[6]. MA Kabir and U Mahbub, "Synchronous detection and digital control of shunt active power filter in power quality improvement,"*Power Energy Conference*, Illinois, pp. 1–5, 2011.

[7]. V Kamatchi Kannan and NRengarajan, "Investigating the performance of photovoltaic based DSTATCOM using Icosϕ

[8]. algorithm"*International Journal of Electrical Power & Energy Systems*, vol. 54, pp. 376-386, 2014.

[9]. G BhubaneswariandMGNair, "Design,Simulation and Analog Circuit Implementation of a Three phase Shunt Active Filter Using Icosϕ

[10]. Algorithm." *IEEE transaction on Power Delivery*,vol. 23, no. 2, pp.1222-1235, 2008.

[11]. B Singh, P Jayaprakash, S Kumar and DPKothari, "Implementation of neural network controlled three-leg VSC and a transformer as three-phase four-wire DSTATCOM," *IEEE Transaction on Industrial Application*, vol. 47, no. 4, pp. 1892–1901,2011.

[12]. B Singh, P Jayaprakash, S Kumar and DP Kothari, "Implementation of Neural-Network-Controlled Three-Leg VSC and a Transformer as Three-Phase Four-Wire DSTATCOM," *IEEE Transactions on Industry Applications*, vol. 47, no. 4, pp. 1892-1901, 2011.

[13]. D Srinivasan, WS Ng and AC Liew, "Neural-network-based signaturerecognition for harmonic source identification,"*IEEE Transactionson Power Delivery*, vol. 21, no.l, pp. 398-405, 2006.

[14]. HC Lin, "Intelligent neural network-based fast power systemharmonic detection,"*IEEE Transactions on Industrial Electronics*, vol.54, no. 1, 2007.

[15]. E Koleva, N Christova and K Velev, "Neural network based approach for quality improvement of orbital arc welding joints," *2010 5th IEEE International Conference Intelligent Systems*, London, pp. 290-295, 2010.

[16]. X Chen, Q Peng, L Han and X Wang, "A Hopfield neural network based algorithm for haplotype assembly from low-quality data," *2014 International Joint Conference on Neural Networks (IJCNN)*, Beijing, pp. 1328-1333, 2014,.

[17]. GB Huang, P Saratchandran and N Sundararajan, "Ageneralized growing and pruning RBF (GGAP-RBF) neural networkfor function approximation,"*IEEE Transactions on Neural Networks*,vol. 16, no. I, pp. 57-67, Jan. 2005.

[18]. H Pomares, I Rojas, M Awad and O Valenzuela, "An enhanced clusteringfunction approximation technique for a radial basis functionneural network,"*Journal of Mathematical and Computer Modelling*,vol. 55, pp. 286-302,2012.

[19]. M. Bortman and M. Aladjem, "A Growing and Pruning Method for Radial Basis Function Networks," *IEEE Transactions on Neural Networks*, vol. 20, no. 6, pp. 1039-1045, 2009.

[20]. H Han, and JF Qiao, "Adaptive computation algorithm forRBF neural network," *IEEE Transactions on Neural Networks andLearning Systems*, vol. 23, no. 2, pp. 342-347, Feb. 2012.

[21]. B Singh and SR Arya, "Back-Propagation Control Algorithm for Power Quality Improvement Using DSTATCOM," *IEEE Transaction on. Industrial. Electronics*, vol. 61, no.3, Mar. 2014.

[22]. Neural Network Toolbox, Version a, The Math Works Inc., 2010.

[23]. RT-Lab Professional. <http://www.opal-rt.com/product/rt-lab-professional>.

A. K. Panda and M. Mangaraj, "DSTATCOM employing hybrid neural network control technique for power quality improvement,"*IET Power Electronics*, vol. 10, no. 4, pp. 480-489, Mar. 2017.

[24]. M. Mangaraj and A. K. Panda, "Performance analysis of DSTATCOM employing various control algorithms,"*IET Generation, Transmission & Distribution*, vol. 11, no. 10, pp. 2643-2653, Jul. 2017.

[25]. M. Mangaraj and A.K Panda, "Modelling and simulation of KHLMS algorithm-based DSTATCOM," *IET Power Electronics*, vol. 12, no. 9, pp. 2304 – 2311, Aug. 2019.

[26]. Mrutyunjaya Mangaraj, Anup Kumar Panda, Trilochan penthia and Asish Ranjan Dash, **"**An Adaptive LMBP Training Based Control Technique for DSTATCOM,**"** *IET Generation, Transmission and Distribution***,** doi: 10.1049/iet-gtd.2018.6295.